

Synthesis and study of the biological activity of thiourea-containing amiridine derivatives as potential multi-target drugs for the treatment of Alzheimer's disease*

G. F. Makhaeva,^{a*} A. N. Proshin,^a N. V. Kovaleva,^a E. V. Rudakova,^a N. P. Boltneva,^a
S. V. Lushchekina,^{a,b} T. Y. Astakhova,^b I. V. Serkov,^a I. P. Kalashnikova,^a and S. O. Bachurin^a

^aInstitute of Physiologically Active Compounds at Federal Research Center of Problems of Chemical Physics and Medicinal Chemistry, Russian Academy of Sciences,

1 Severny proezd, 142432 Chernogolovka, Moscow Region, Russian Federation

^bN. M. Emanuel Institute of Biochemical Physics, Russian Academy of Sciences,
4 ul. Kosygina, 119334 Moscow, Russian Federation.

E-mail: gmakh@ipac.ac.ru

The synthesis of new compounds based on the domestic drug amiridine modified with derivatives of *N*-mono- and *N,N*-disubstituted thiourea is described. The compounds were investigated for the anticholinesterase and antioxidant activities and for the ability to inhibit the self-aggregation of β -amyloid ($A\beta_{42}$). The structure–activity relationships were analyzed. The observed effects were consistent with the results of molecular docking of the compounds into cholinesterases and $A\beta_{42}$. The compounds that effectively inhibit butyrylcholinesterase and demonstrate high antioxidant and antiaggregant activities were identified. The results show promise for further development of this class of compounds as potential multifunctional agents for the treatment of Alzheimer's disease.

Key words: amiridine, thiourea, (het)arylalkylamines, acetylcholinesterase, butyrylcholinesterase, carboxylesterase, antioxidants, β -amyloid, neurodegenerative diseases, Alzheimer's disease.

Alzheimer's disease (AD) is the most frequent type of dementia in elderly persons, which is characterized by persistent decrease in cognitive functions and memory down to complete loss of personality. The lack of effective therapy of AD is largely due to the multifactorial nature of the disease. In clinical practice AD is treated, most often, with four drugs, including three cholinesterase inhibitors (donepezil, galantamine, and rivastigmine) and one NMDA receptor antagonist (memantine)¹ (tacrine, the first anticholinesterase drug approved by the Food and Drug Administration (FDA, USA), was later withdrawn because of hepatotoxicity). These drugs counterbalance the symptoms of the disease, that is, the lost cognitive function, but cannot stop progression of the proper neurodegenerative process, leading to complete disability and disorientation of patients. In view of the serious medical and social problems associated with AD, the search for new effec-

tive drugs for the treatment of this disease is a relevant task of modern medicinal chemistry.

Development of Alzheimer's disease is a multifactorial process involving dozens of molecular mechanisms. Therefore, an efficient approach is the design of multifunctional, multi-target molecules that can synergistically affect several targets and/or processes involved in the pathogenesis of the disease. Characteristic features of the AD pathogenesis are dysfunction of neurotransmitter systems, deposition of aberrant proteins (β -amyloid and τ -protein), oxidative stress, mitochondrial dysfunction, loss of synapses, and death of neurons, especially cholinergic neurons.^{2,3}

Currently, the development of cholinesterase inhibitors with additional antioxidant and antiaggregant properties is considered to be a promising approach to the design of multifunctional molecules. Drugs that are already used in practice often serve as the base for such multifunctional molecules. For this purpose, the drug molecules are chemically modified in an appropriate way, being endowed with neuroprotective and disease-modifying properties.^{4–8}

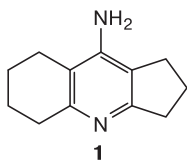
* Based on the materials of the V Russian Conference on Medicinal Chemistry with international participation "MedChem-Russia 2021" (May 16–19, 2022, Volgograd, Russia).

In this study, as the base molecule to be modified, we chose amiridine **1**, a pharmacological drug developed in the USSR in the mid-1980s and officially approved for the treatment of AD and some other neurological disorders.⁹ Amiridine, 9-amino-2,3,5,6,7,8-hexahydro-1*H*-cyclopenta[*b*]quinoline (also known as ipidacrine, NIK-247, neuromidin, Axamon, Ipigrix), is an anticholinesterase drug, widely used in Russia and in some other Eastern Europe countries for the treatment of AD and several other disorders of the central and peripheral nervous systems.^{10–14} Apart from the reversible inhibition of acetylcholinesterase (AChE) and butyrylcholinesterase (BChE) with selectivity towards BChE, amiridine has a broad range of biological activities,^{15,16} which was addressed in our previous publication.¹⁷

The molecule of amiridine **1** contains a 4-amino-pyridine moiety and is structurally similar to tacrine (9-amino-1,2,3,4-tetrahydroacridine). Unlike the latter, amiridine has much less peripheral and central cholinergic side effects, no hepatotoxicity, and a wider therapeutic window.^{15,18} However, the amiridine molecule is less reactive than tacrine; therefore, virtually no data on amiridine derivatives are available in the literature, and functionalization of the amiridine molecule at the amino group with retention of the unique amiridine skeleton is a challenging task.^{19,20}

Recently,¹⁷ we carried out the first amiridine functionalization at the acyclic nitrogen atom *via* acylation with chloroacetic acid. The amiridine chloroacetamide thus formed was reacted with piperazine, which resulted in the synthesis of several hybrid structures promising as potential multifunctional agents for the treatment of AD. The reaction of amiridine chloroacetamide with diaminoalkanes afforded a number of amiridine homodimers with bis-*N*-acylalkylene spacer.²¹ We also developed a method for amiridine functionalization with thiophosgene to give 9-isothiocyanato-2,3,5,6,7,8-hexahydro-1*H*-cyclopenta[*b*]quinoline (**2**), amiridine isothiocyanate, which allowed the synthesis of amiridine homodimers with a bis-*N*-thiourea-alkylene spacer,²¹ which demonstrated, apart from cholinesterase inhibition, a high antioxidant potential and antiaggregant activity against β -amyloid.

In this study, amiridine isothiocyanate **2** was modified by a number of (het)arylalkylamines, since previously we have shown that compounds containing dibenzylamine²² and isothiourea²³ moieties possess neuroprotective properties. The presence of the thiourea moiety suggests a good antioxidant activity of the products,^{21,24–26} while the presence of arylalkylamine



groups in the thiourea-containing amiridine derivatives may imply a potential ability to inhibit β -amyloid self-aggregation.^{27,28} In view of the cholinergic neurotransmission disorder inherent in AD and the key role of oxidative stress and β -amyloid aggregation in the origin and progression of AD, we studied the esterase profile²⁹ of the synthesized compounds (the inhibitory activity against AChE, BChE, and structurally related carboxylesterase (CES)), their intrinsic antioxidant activity, and the ability to inhibit the aggregation of β -amyloid. The observed structure–activity relationships were interpreted using molecular docking methods.

Synthesis of compounds. The reaction of amiridine isothiocyanate **2**, which was synthesized by the reaction of amiridine **1** with thiophene,²¹ with equimolar amounts of primary and secondary (het)arylalkylamines in diethyl ether at room temperature afforded amiridine derivatives containing *N*-monosubstituted (**3a–e**) and *N,N*-disubstituted thioureas (**4a–d**) (Scheme 1).

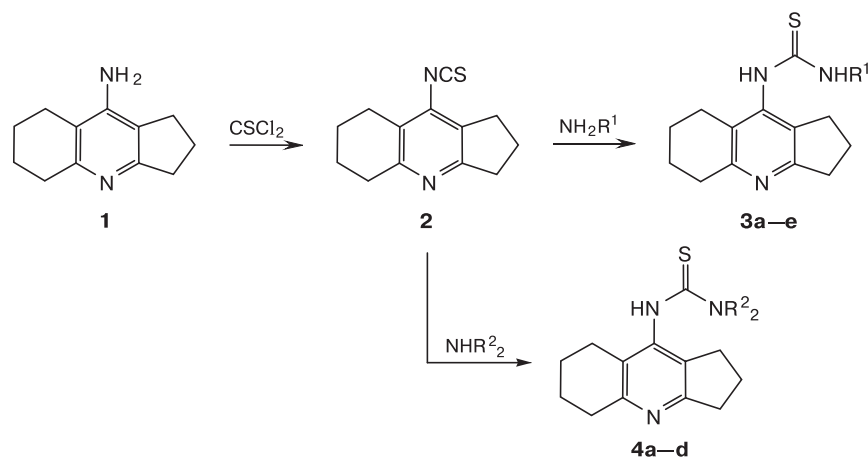
Study of the esterase profile of amiridine derivatives 3 and 4 showed (Table 1) that they inhibit AChE rather weakly (the maximum inhibition is 30% at a concentration of 20 $\mu\text{mol L}^{-1}$, *i.e.*, $\text{IC}_{50} > 70 \mu\text{mol L}^{-1}$) and inhibit BChE much more efficiently, with IC_{50} being in the micromolar range.

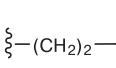
Analysis of the structure–activity relationships provides the conclusion that compounds **3a–c** with one substituent at the nitrogen atom of the *N*-thiourea moiety inhibit BChE more efficiently than disubstituted derivatives **4a–c**. It can also be seen that the replacement of phenylalkylamine (**3b**) by pyridylalkylamine (**3e**) has an adverse effect on the anti-ChE activity. It is of interest that in the case of disubstituted thioureas, the replacement of phenylalkylamine (**4a**) with pyridylalkylamine (**4d**) enhances the inhibition of BChE.

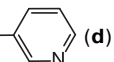
Low inhibition of CES, an enzyme that hydrolyzes many medicinal drugs with ester groups, is a good feature of the synthesized products, as this decreases the probability of undesirable drug interactions in the case where they are used in the AD therapy.

Molecular docking into AChE and BChE. The estimation of pK_a value for the amiridine moiety in these compounds carried out using two different programs (see Experimental) resulted in the values from 6 to 7.6, indicating that the compounds can exist in both neutral and protonated states under experimental conditions. Meanwhile, according to the results of molecular docking of monosubstituted compounds **3**, the protonated state of the amiridine moiety has almost no effect on the position of inhibitors in the AChE channel (Fig. 1, *a*). In the protonated state, the amiridine moiety is hydrogen-bonded to the oxygen atom of the Trp86

Scheme 1



3: $\text{R}^1 = \text{Bn}$ (a), $(\text{CH}_2)_2\text{Ph}$ (b), $(\text{CH}_2)_3\text{Ph}$ (c), 3,4,5-(MeO) $_3\text{C}_6\text{H}_2\text{CH}_2$ (d), $\xi-(\text{CH}_2)_2$ - (e)

4: $\text{R}^2 = \text{Bn}$ (a), $(\text{CH}_2)_2\text{Ph}$ (b), $(\text{CH}_2)_3\text{Ph}$ (c), $\xi-\text{CH}_2$ - (d)

(W86) backbone, while in the neutral state, it is bound to the backbone through a bridging water molecule, as was shown in our previous study¹⁷ using molecular dynamic simulation. In addition, the position of the

inhibitor in the active site is stabilized by hydrogen bonds with the Tyr124 (Y124) and Tyr341 (Y341) side chains, which requires disruption of the planarity of the amiridine moiety. Binding to the peripheral anionic

Table 1. Biological activity of compounds 3a–e and 4a–d: esterase profile, β -amyloid self-aggregation inhibition, and antioxidant properties

Compound	Inhibitory activity			$\text{A}\beta_{42}$ self-aggregation inhibition (%) ^b	Antioxidant properties	
	AChE ^a (%)	BChE IC ₅₀ /μmol L ⁻¹	CES ^a (%)		ABTS/TEAC ^c (IC ₅₀ /μmol L ⁻¹)	FRAP/TE ^d
3a	27.2±1.2	2.34±0.21	6.2±0.1	23.7±1.8	0.8±0.03 (26.5±1.8)	0.24±0.01
3b	29.7±0.6	2.90±0.21	9.9±0.8	35.8±3.2	0.3±0.02 (51.3±1.9)	0.07±0.01
3c	24.6±0.4	1.82±0.17	11.2±1.0	40.6±3.6	0.6±0.03 (34.2±1.6)	0.21±0.02
3d	7.8±0.8	11.2±0.1	2.5±0.3	36.4±2.9	0.65±0.03 (29.7±1.5)	0.31±0.01
3e	15.2±0.8	9.21±0.77	16.0±1.2	31.9±2.5	0.8±0.03 (22.7±1.3)	0.10±0.02
4a	20.5±0.8	11.2±0.3	23.0±1.9	39.1±3.5	1.1±0.06 (14.2±0.8)	0.03±0.01
4b	20.9±0.3	5.56±0.05	7.9±0.6	58.3±4.6	0.75±0.04 (23.8±1.5)	— ^e
4c	12.9±0.8	5.84±0.19	4.5±0.3	36.5±2.5	1.0±0.04 (19.5±0.8)	0.14±0.01
4d	26.5±1.9	4.40±0.16	8.7±0.7	27.5±2.4	0.9±0.04 (20.4±1.0)	0.12±0.02
Amiridine (1)	85.4±0.2 ^f	0.272±0.015	2.7±0.5	6.4±0.5	0.04±0.003 (— ^g)	— ^e
BNPP	— ^e	— ^e	99.1±0.93 ^h	— ^g	— ^g	— ^g
Myricetin	— ^g	— ^g	— ^g	74.7±5.2	— ^g	— ^g
Trolox	— ^g	— ^g	— ^g	— ^g	1.0 (20.1±1.2)	1.0

Note. The data are expressed as mean ± SEM, $n = 3$.

^a The concentration of the compound is 20 μmol L⁻¹.

^b Inhibition of self-aggregation of $\text{A}\beta_{42}$ (50 μmol L⁻¹) by the test compound in the concentration of 100 μmol L⁻¹.

^c TEAC is the trolox equivalent antioxidant capacity found as the ratio of the slopes of the dependences for the decrease in the ABTS^{•+} concentration on the concentrations of the test compound and trolox.

^d TE is the trolox equivalent characterizing the iron-reducing activity defined as the ratio of trolox and test compound concentrations that induce equal effects.

^e No activity.

^f IC₅₀ is 4.44±0.36 μmol L⁻¹.

^g Not determined.

^h IC₅₀ is 1.80 ± 0.11 μmol L⁻¹.

site (PAS) is insignificant in comparison with that for amiridine derivatives studied previously.¹⁷

Owing to larger active site channel in BChE compared to AChE, inhibitors can occupy more diverse positions in the former. While comparing the positions of compounds **3a** and **4a** in the BChE active site (Fig. 1, *b*), it can be seen that **3a** has a larger number of specific interactions with BChE than **4a**: the amiridine moiety of **3a** is hydrogen-bonded to the backbone oxygen atom of the His438 (H438) catalytic residue and is linked to the Trp82 (W82) indole ring by π -cationic interactions, and the amino group is hydrogen-bonded to the Asp70 (D70) side chain. This accounts for the higher inhibitory activity of the monosubstituted derivative **3a** compared to disubstituted compound **4a**, in which the amiridine moiety is hydrogen-bonded to the oxygen atom of Leu286 (L286), while the sulfur atom is located in the oxyanion hole.

Compounds **3** and **4** are relatively weak AChE inhibitors. Nevertheless, considering the possibility of binding of monosubstituted compounds **3** in the active site channel of AChE (see Fig. 1, *a*), we evaluated the possibility of competitive displacement of propidium iodide, a specific PAS ligand, by these compounds using the fluorescence method.³⁰ The experiment showed that compounds **3** and **4** cannot displace propidium iodide, which is in line with the molecular docking results.

The inhibitory action of the test compounds on the self-aggregation of β -amyloid (1-42) ($A\beta_{42}$) was determined by the fluorescence method using thioflavine T.^{31,32} This method is widely used for primary screening to identify active compounds. The results on the inhibition of $A\beta_{42}$ self-aggregation by compounds **3** and **4** (see Table 1) show that amiridine derivatives **3a–e** inhibit the self-aggregation of $A\beta_{42}$ in the 23–40% range, whereas *N,N*-disubstituted compounds **4a–d** show a higher degree of inhibition, ranging from 27 to 58%. A comparison of compounds **3a,b** and **4a,b** with benzyl and phenethyl substituents shows that the anti-aggregant activity increases on going from *N*-monosubstituted to *N,N*-disubstituted derivatives. Compound **4b** with two phenethyl substituents showed the highest antiaggregant activity ($58.3 \pm 4.6\%$) among all studied amiridine derivatives.

Molecular docking into $A\beta_{42}$. Since study of the $A\beta_{42}$ self-aggregation inhibition by fluorescence method using thioflavine T reveals the formation of β -folded structures that form toxic $A\beta_{42}$ oligomers and fibrils, molecular docking was carried out using the α -helical soluble $A\beta_{42}$ monomer as the target. The available structure PDB ID 1IYT was obtained by NMR spectroscopy and contained ten conformations of the monomer. This structure is actively used as a model for the soluble monomeric form of $A\beta_{42}$ for molecular docking. However, in the relevant publications, it is most often

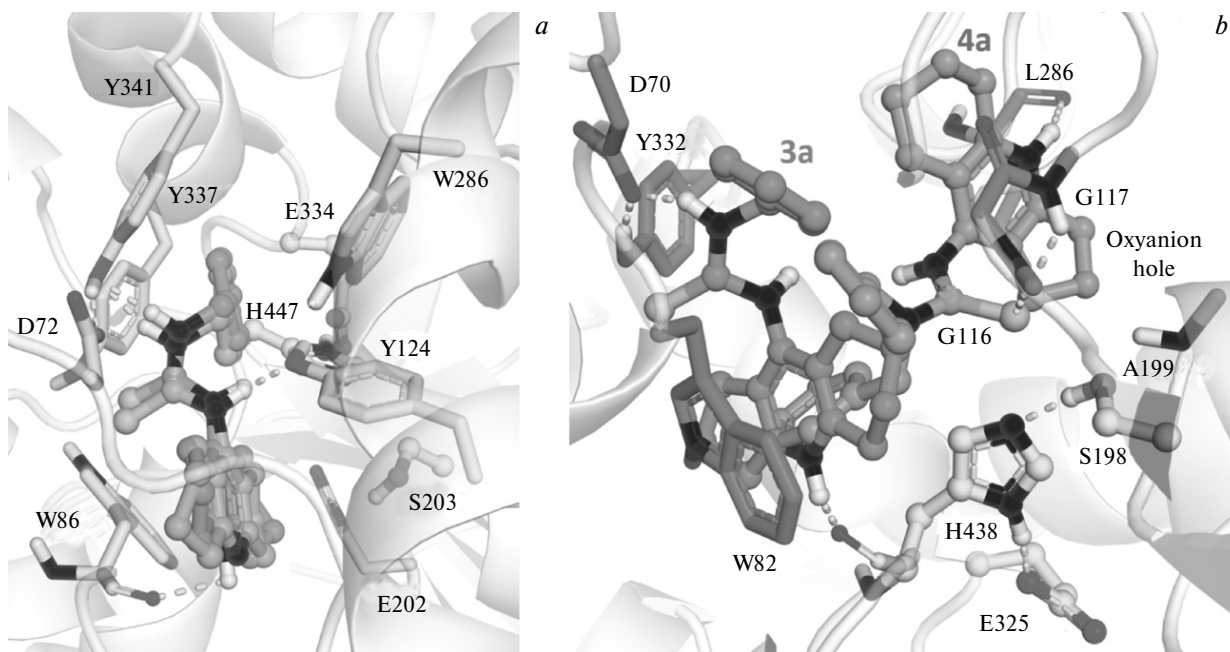


Fig. 1. *a.* Docking of compound **3a** into the AChE active site (the carbon atoms of the neutral form are shown in pink; those of the protonated form are in green). *b.* Position of compounds **3a** and **4a** in the BChE active site based on the results of molecular docking (the carbon atoms of compound **3a** are shown in green, those of compound **4a** are shown in light blue).

indicated (or follows from the presented results) that only one out of the ten conformers was used: either the first or the sixth one, which has the least deviation from other conformers,³³ or it is not clearly indicated which particular conformer was taken, and it can only be surmised that this was the first conformer.

In this study, we carried out molecular docking using all conformers of A β ₄₂ as the targets using mono-substituted and disubstituted analogs that differed most strongly in the ability to inhibit the self-aggregation of A β ₄₂ (pairs **3a**, **4a** and **3b**, **4b**) as ligands; protonated and neutral forms of compounds were also considered.

According to the molecular docking data, binding of compounds to various conformers of A β ₄₂ considerably differed (Table 2). This difference is clearly seen in Fig. 2, *a* in relation to compound **4b**. It is noteworthy that the position of **4b** in the vicinity of the *N*-terminal region found upon docking into the first A β ₄₂ conformer differs appreciably from the positions in the vicinity of the turn segment of the *C*-terminal peptide obtained for all other conformers. With all differences of the molecular docking results for different A β ₄₂ conformers, there is a consistent trend towards stronger binding of compounds **4** compared to **3** regarding both single conformers (with rare exceptions) and the average and minimum binding energies (see Table 2). The strongest binding among all positions was found for the protonated form of compound **4b** and for the third conformer of A β ₄₂. Figure 2, *b* depicts binding of compounds **3b** and **4b** in the hydrophobic *C*-terminal residue and turn segment, which are A β ₄₂ regions critical for the conformational transition and initial nucleation for fibril formation.³⁴ The interactions between the peptide and the ligand are non-specific and

hydrophobic (see Fig. 2, *b*); nevertheless, they ensure identical positions of both compounds, with the second phenethyl substituent of compound **4b** providing a better binding due to the hydrophobic contacts with the Val24 (V24) and Phe20 (F20) side chains. Stronger binding of compound **4b** reflects the experimentally observed higher inhibitory activity against the β -amyloid self-aggregation compared to compounds **4a** and **3b**. Generally, the introduction of hydrophobic arylalkyl substituents able to interact with the hydrophobic regions of the soluble A β ₄₂ monomer and to stabilize its α -helical conformation significantly increases the ability to inhibit self-aggregation compared to the initial amiridine pharmacophore.

Analysis of the results of molecular docking with higher binding energy did not reveal positions in the vicinity of the HHQK domain, which is important for oligomerization and appearance of neurotoxicity of A β ₄₂.^{35,36} Binding to this domain was found for positions with lower docking energies (see Fig. 2, *b*). It can be seen that for most similar conformers (the fourth and eighth conformers of A β ₄₂, RMSD of 1.3 Å, Table 3), all of the obtained docking positions differ to a much greater extent than those for the most different conformers (see Table 3, the RMSD between the fourth and tenth conformer of A β ₄₂ is 4.9 Å), which is additional evidence for the considerable contribution of the conformational mobility of A β ₄₂ to the interaction with inhibitors. The molecular docking using different A β ₄₂ conformers provides definite structural information necessary for the subsequent development of disease-modifying drugs for AD therapy; however, complete description can be obtained only using molecular dynamics techniques if sufficient computational resources are available.

Table 2. Binding energies ($-E_b/\text{kcal mol}^{-1}$) for the neutral and protonated forms of compounds **3a,b** and **4a,b** to conformers 1–10 of the soluble form of A β ₄₂ monomer according to the molecular docking results

Compound	Conformer of A β ₄₂										$-E_b^{\text{av}}$	$-E_b^{\text{min}}$
	1	2	3	4	5	6	7	8	9	10		
Neutral form												
3a	5.4	5.5	5.4	5.2	5.1	5.3	5.2	5.5	5.5	5.4	5.3	5.5
4a	5.5	5.5	5.6	5.5	5.9	5.5	5.1	5.7	5.6	5.6	5.5	5.9
3b	5.2	5.5	5.2	5.2	5.1	5.2	5.2	5.4	5.6	5.2	5.3	5.6
4b	5.6	5.6	6	5.7	5.2	5.5	5	5.7	5.7	5.6	5.5	6
Protonated form												
3a	5.4	5.3	5.4	5.4	5.1	5.4	5.3	5.8	5.6	5.4	5.4	5.8
4a	5.7	5.8	6	5.4	5.7	5.3	5.4	5.9	5.7	5.4	5.6	6
3b	5.3	5.2	5.4	5.3	5.3	5.4	5.3	5.6	5.6	5.4	5.4	5.6
4b	5.7	5.6	6.1	5.3	5.2	5.7	5.5	5.8	6.1	5.7	5.6	6.1

Note. E_b^{av} and E_b^{min} are the average and minimum binding energies of compounds **3a,b** and **4a,b** to all conformers of A β ₄₂.

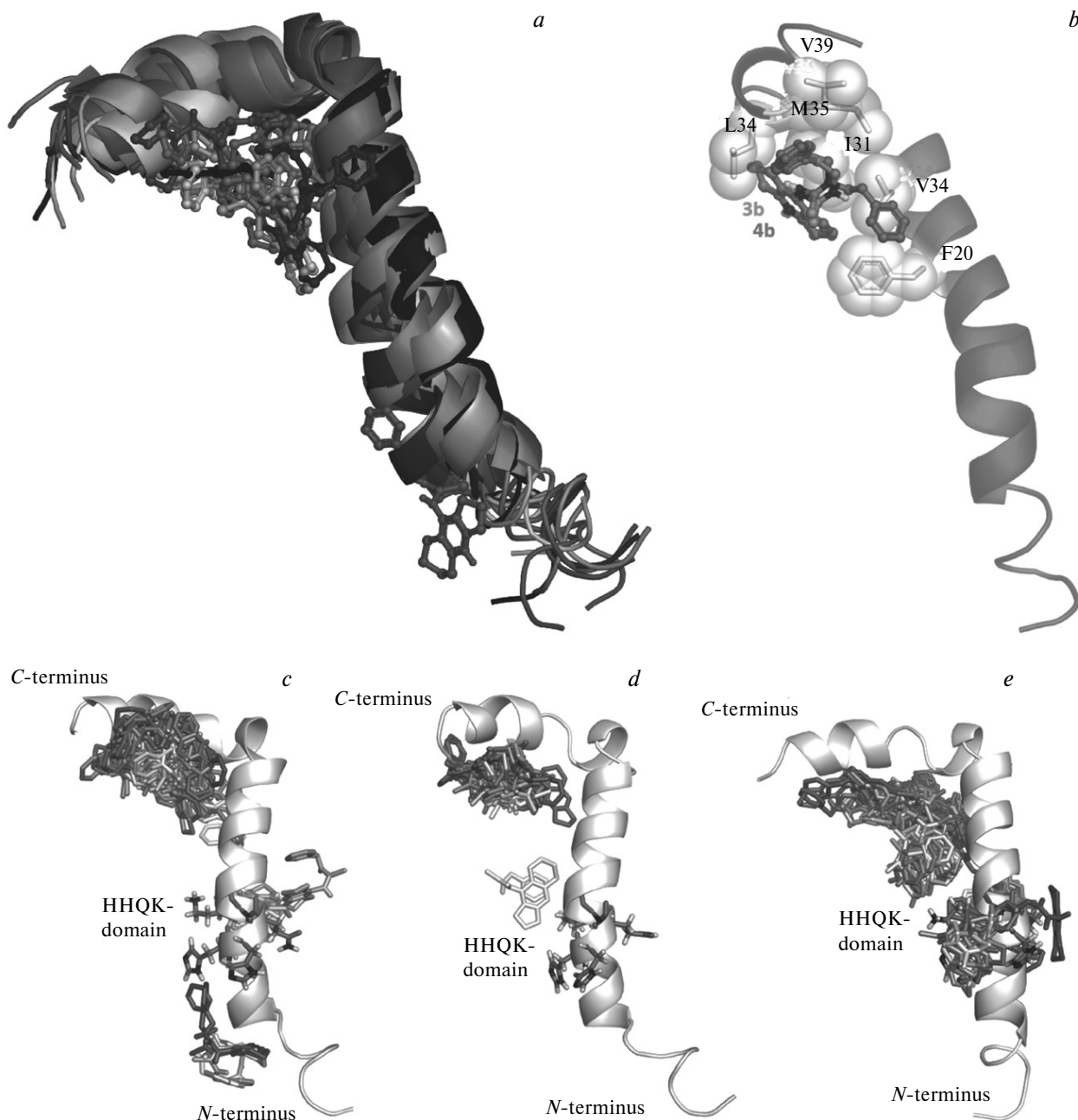


Fig. 2. *a.* Results of molecular docking of compound **4b** with all conformers of the α -helical soluble monomer form of $A\beta_{42}$ (PDB ID 1IYT) (the color gradually changes from red through white to blue from the first to the tenth $A\beta_{42}$ conformer). *b.* Binding of compounds of **3b** (the carbon atoms are shown in orange) and **4b** (the carbon atoms are shown in turquoise) to the third conformer of $A\beta_{42}$. *c–e.* All positions found from the results of molecular docking (the color gradually changes from red to white as binding is being weakened) for the eighth (*c*), fourth (*d*), and tenth (*e*) conformers of $A\beta_{42}$. Green color shows the carbon atoms of the side chains of the His13, His14, Gln15, and Lys16 residues.

The intrinsic antioxidant activity of the compounds was evaluated using two standard methods, one based on the radical scavenging properties in the ABTS assay, which measures the ability of test compounds to scavenge the model ($ABTS^{\bullet+}$) radical cation,³⁷ and one based on the reducing ability of the compounds in the

FRAP (ferric reducing antioxidant power) assay, which measures the ability of test compounds to reduce Fe^{3+} complex to Fe^{2+} complex.³⁸

The results showed (see Table 1) that unlike parent amiridine **1**, all the amiridine derivatives with *N*-substituted thioureas show high radical-scavenging activity

Table 3. Root mean-square deviation (RMSD/Å) between the conformers of Aβ₄₂ calculated for heavy atom coordinates after alignment

Conformer Aβ ₄₂	Conformer Aβ ₄₂									
	1	2	3	4	5	6	7	8	9	10
1	—	2.6	2.1	3.6	3.2	3.1	2.6	2.8	2.7	2.7
2	2.6	—	2.6	2	2.2	3.8	2.8	1.4	1.6	3.9
3	2.1	2.6	—	3.1	2.8	2.8	2.9	2.5	2.5	2.7
4	3.6	2	3.1	—	2.1	4.8	4	1.3	2.5	4.9
5	3.2	2.2	2.8	2.1	—	4.4	4	2.1	2.3	4.2
6	3.1	3.8	2.8	4.8	4.4	—	3.2	4.2	3.8	1.5
7	2.6	2.8	2.9	4	4	3.2	—	3.2	3	2.8
8	2.8	1.4	2.5	1.3	2.1	4.2	3.2	—	1.7	4.2
9	2.7	1.6	2.5	2.5	2.3	3.8	3	1.7	—	3.6
10	2.7	3.9	2.7	4.9	4.2	1.5	2.8	4.2	3.6	—

in the ABTS assay, comparable to that of trolox. The activity of compound **3a** with *N*-benzyl substituent (TEAC = 0.8) is close to the trolox activity; analogs **3b** and **3c** with longer alkyl chains are less active (by 2.7 and 1.3 times, respectively). "Doubling" of the arylalkyl substituent at the thiourea nitrogen atom generally promotes an increase in the ABTS^{•+}-scavenging activity: **4a** > **3a**; **4b** > **3b**; **4c** > **3c**. The highest radical-scavenging activity, equal to that of trolox, was found for **4a** and **4c**.

One of indications of the potential antioxidant properties of a compound is the reducing ability,³⁹ which is usually measured by reduction of model metal complexes. In the FRAP assay (see Table 1), amiridine derivatives with *N*-substituted thioureas possess a moderate iron-reducing activity, with "doubling" of the substituent at the thiourea nitrogen atom decreasing the ability to reduce Fe³⁺ ions (*cf.* data for **3a–c** and **4a–c**, Table 1). The highest activity was found for monosubstituted derivative **3d** containing three methoxy groups, which enhance the oxidative potential of the compound.

Thus, the study shows that the thiourea amiridine derivatives **3** and **4**, which we synthesized, selectively inhibit BChE with IC₅₀ values being in the micromolar range; higher activity was found for compounds with *N*-monosubstituted thiourea. These compounds effectively inhibit the Aβ₄₂ self-aggregation as a result of hydrophobic interactions with the domains critical for the conformational transition and early nucleation to give fibrils; derivatives with *N,N*-disubstituted thioureas are more active (compound **4b** with two phenethyl substituents is the most active; when present in concentration of 100 μmol L⁻¹, it inhibits the self-aggregation of Aβ₄₂ by 58.3±4.6%). The results of molecular docking into BChE and Aβ₄₂ account for the observed

effects and show the importance of using different conformations of Aβ₄₂ for the molecular modeling of self-aggregation inhibition. *N,N*-Disubstituted derivatives **4** also show higher radical-scavenging activity in the ABTS assay (the activity of **4a,c** is equal to that of trolox). However, doubling of substituents at the thiourea nitrogen atom decreases the ability of conjugates to reduce Fe³⁺ ions. The results show promise for further development of this class of compounds as potential multifunctional drugs for the treatment of AD and selective BChE inhibitors with Aβ₄₂ antiaggregant activity and antioxidant properties.

Experimental

The synthesis and biochemical studies were carried out using commercially available chemicals (Sigma, USA), which were used as received unless indicated otherwise.

Compound **2** was synthesized from amiridine manufactured by PIK Farma (Russia).

The solvents were made absolute by standard procedures. The reactions were monitored by thin layer chromatography on Silufol-UV254 plates and by NMR spectroscopy. The melting points were determined on a Stuart SMP10 device (Bibby Scientific, UK) and were not corrected. The ¹H and ¹³C NMR spectra were recorded in CDCl₃ on a Bruker DPX-200 spectrometer (Germany) at 28 °C (Me₄Si as the internal standard). Elemental analysis was done on a Carlo-Erba ER-20 CHN-analyzer (France).

9-Isothiocyano-2,3,5,6,7,8-hexahydro-1*H*-cyclopenta[*b*]quinoline (2).²¹ A solution of thiophosgene (2 mL, 26 mmol) in chloroform (10 mL) was added dropwise to a vigorously stirred mixture of amiridine **1** (5 g, 26 mmol) in chloroform (25 mL) and NaHCO₃ (3 g) in water (25 mL) cooled to 0 °C. The reaction was monitored by ¹H NMR spectroscopy; stirring was continued for 5–7 h until the initial amine was completely consumed (broadened proton singlet of the amino group at 4 ppm). After completion of the reaction, the

organic phase was washed with water (2×50 mL) and a saturated solution of NaCl and dried with anhydrous sodium sulfate. The solvent was evaporated, the residue was extracted with diethyl ether (2×50 mL), and the solvent was evaporated to give 1.4 g (22%) of product **2**. Brown crystals. m.p. 103–105 °C. ¹H NMR, δ: 1.75–2.03 (m, 4 H, CH₂CH₂); 2.12–2.51 (m, 2 H, CH₂); 2.80 (br.s, 2 H, CH₂); 3.10 (t, 2 H, CH₂, *J* = 7.5 Hz); 3.21–3.36 (m, 2 H, CH₂); 3.10 (t, 2 H, CH₂, *J* = 7.7 Hz). ¹³C NMR (CDCl₃), δ: 21.40, 24.17, 25.16, 27.18, 31.27, 32.46, 35.42, 129.60, 135.98, 141.28, 144.48 (C=S), 156.96, 163.57. Found (%): C, 67.54; H, 6.013; N, 12.26. C₁₃H₁₄N₂S. Calculated (%): C, 67.79; H, 6.13; N, 12.16.

Synthesis of amiridine derivatives with mono- (3) and di-substituted (4) thioureas (general procedure). A solution of the specified substituted amine (0.5 mmol) in diethyl ether (3 mL) was added with stirring to a solution of compound **2** (115 mg, 0.5 mmol) in diethyl ether (3 mL). The precipitate was filtered off and recrystallized from propan-2-ol (5 mL).

1-Benzyl-3-(2,3,5,6,7,8-hexahydro-1*H*-cyclopenta[*b*]quinolin-9-yl)thiourea (3a). White crystals. Yield 72%. M.p. 178–180 °C. ¹H NMR, δ: 1.55–1.83 (m, 4 H, CH₂CH₂); 1.85–2.11 (m, 2 H, CH₂); 2.38–2.61 (m, 2 H, CH₂); 2.61–3.05 (m, 6 H, CH₂); 4.72 (d, 2 H, NCH₂, *J* = 4.9 Hz); 6.22 (br.s, 1 H, NH); 7.09 (br.s, 1 H, NH); 7.20 (br.s, 5 H, H_{Ar}). Found (%): C, 71.39; H, 6.81; N, 12.56. C₂₀H₂₃N₃S. Calculated (%): C, 71.18; H, 6.87; N, 12.45.

1-(2,3,5,6,7,8-Hexahydro-1*H*-cyclopenta[*b*]quinolin-9-yl)-3-phenylthiourea (3b). Light gray crystals. Yield 74%, m.p. 194–196 °C. ¹H NMR, δ: 1.62–1.92 (m, 4 H, CH₂CH₂); 1.99 (pent, 2 H, CH₂, *J* = 7.88 Hz); 2.38–2.53 (m, 2 H, CH₂); 2.60 (t, 2 H, ArCH₂, *J* = 7.5 Hz); 2.81–3.05 (m, 6 H, CH₂); 3.88 (q, 2 H, NCH₂, *J* = 6.2 Hz); 5.50 (br.s, 1 H, NH); 7.05–7.12 (m, 2 H, H_{Ar}); 7.20–7.28 (m, 3 H, H_{Ar}), 7.75 (br.s, 1 H, NH). Found (%): C, 71.71; H, 7.11; N, 12.06. C₂₁H₂₅N₃S. Calculated (%): C, 71.75; H, 7.17; N, 11.95.

1-(2,3,5,6,7,8-Hexahydro-1*H*-cyclopenta[*b*]quinolin-9-yl)-3-(3-phenylpropyl)thiourea (3c). Light gray crystals. Yield 68%, m.p. 178–180 °C. ¹H NMR, δ: 1.70–1.83 (m, 4 H, CH₂CH₂); 1.99 (pent, 2 H, CH₂CH₂CH₂, *J* = 7.6 Hz); 2.09 (pent, 2 H, CH₂, *J* = 7.6 Hz); 2.54–2.72 (m, 4 H, CH₂); 2.79 (t, 2 H, ArCH₂, *J* = 7.3 Hz); 2.86–3.04 (m, 4 H, CH₂); 3.67 (q, 2 H, NCH₂, *J* = 6.5 Hz); 5.50 (br.s, 1 H, NH); 7.00–7.41 (m, 5 H, H_{Ar}); 7.50 (br.s, 1 H, NH). Found (%): C, 72.37; H, 7.56; N, 11.40. C₂₂H₂₇N₃S. Calculated (%): C, 72.29; H, 7.45; N, 11.50.

1-(2,3,5,6,7,8-Hexahydro-1*H*-cyclopenta[*b*]quinolin-9-yl)-3-(3,4,5-trimethoxybenzyl)thiourea (3d). Yellowish crystals. Yield 66%, m.p. 183–185 °C. ¹H NMR, δ: 1.52–1.83 (m, 4 H, CH₂CH₂); 1.85–2.14 (m, 2 H, CH₂); 2.40–2.68 (m, 2 H, CH₂); 2.68–3.02 (m, 6 H, CH₂); 3.70 (s, 3 H, OCH₃); 3.72 (s, 6 H, OCH₃); 4.72 (d, 2 H, NCH₂, *J* = 3.3 Hz); 6.32 (br.s, 1 H, NH); 6.49 (s, 2 H, H_{Ar}); 7.11 (br.s, 1 H, NH). Found (%): C, 64.51; H, 6.68; N, 9.65. C₂₃H₂₉N₃O₃S. Calculated (%): C, 64.61; H, 6.84; N, 9.83.

1-(2,3,5,6,7,8-Hexahydro-1*H*-cyclopenta[*b*]quinolin-9-yl)-3-[2-(pyridin-2-yl)ethyl]thiourea (3e). Yellow crystals.

Yield 70%, m.p. 146–148 °C. ¹H NMR, δ: 1.55–1.88 (m, 4 H, CH₂CH₂); 1.98 (pent, 2 H, CH₂, *J* = 7.5 Hz); 2.50–2.67 (m, 2 H, CH₂); 2.74 (t, 2 H, ArCH₂, *J* = 7.3 Hz); 2.85–3.05 (m, 6 H, CH₂); 4.04 (q, 2 H, NCH₂, *J* = 5.5 Hz); 6.98–7.25 (m, 2 H, pyridyl); 7.20–7.28 (m, 3 H, H_{Ar}); 7.60 (t, 1 H, pyridyl, *J* = 7.6 Hz); 7.81 (br.s, 2 H, NH); 7.95 (d, 1 H, pyridyl, *J* = 7.8 Hz). Found (%): C, 68.025; H, 6.99; N, 15.84. C₂₀H₂₄N₄S. Calculated (%): C, 68.15; H, 6.86; N, 15.89.

1,1-Dibenzyl-3-(2,3,5,6,7,8-hexahydro-1*H*-cyclopenta[*b*]quinolin-9-yl)thiourea (4a). White crystals. Yield 76%, m.p. 168–170 °C. ¹H NMR, δ: 1.55–1.89 (m, 4 H, CH₂CH₂); 1.89–2.17 (m, 2 H, CH₂); 2.17–2.66 (m, 2 H, CH₂); 2.66–3.26 (m, 6 H, CH₂); 5.10 (br.s, 4 H, N(CH₂)₂); 6.59 (br.s, 1 H, NH); 7.09 (br.s, 1 H, NH); 7.29–7.61 (m, 10 H, H_{Ar}). Found (%): C, 75.66; H, 6.68; N, 9.78. C₂₇H₂₉N₃S. Calculated (%): C, 75.84; H, 6.84; N, 9.83.

3-(2,3,5,6,7,8-Hexahydro-1*H*-cyclopenta[*b*]quinolin-9-yl)-1,1-diphenylethylthiourea (4b). White crystals. Yield 65%, m.p. 148–150 °C. ¹H NMR, δ: 1.62–1.96 (m, 4 H, CH₂CH₂); 1.99–2.18 (m, 2 H, CH₂); 2.68–3.29 (m, 12 H, CH₂); 3.65–4.05 (m, 4 H, N(CH₂)₂); 6.31 (br.s, 1 H, NH); 7.05–7.52 (m, 10 H, H_{Ar}). Found (%): C, 76.31; H, 7.30; N, 9.08. C₂₉H₃₃N₃S. Calculated (%): C, 76.44; H, 7.30; N, 9.22.

3-(2,3,5,6,7,8-Hexahydro-1*H*-cyclopenta[*b*]quinolin-9-yl)-1,1-bis(3-phenylpropyl)thiourea (4c). White crystals. Yield 61%, m.p. 175–177 °C. ¹H NMR, δ: 1.61–1.93 (m, 4 H, CH₂CH₂); 1.93–2.22 (m, 6 H, 2 CH₂CH₂CH₂ and CH₂CH₂CH₂); 2.27–3.10 (m, 12 H, 2 (CH₂)_{Ar} and 4 CH₂); 3.55–3.84 (m, 4 H, N(CH₂)₂); 6.08 (br.s, 1 H, NH); 7.02–7.41 (m, 10 H, H_{Ar}). Found (%): C, 77.09; H, 7.86; N, 8.79. C₃₁H₃₇N₃S. Calculated (%): C, 76.97; H, 7.71; N, 8.69.

3-(2,3,5,6,7,8-Hexahydro-1*H*-cyclopenta[*b*]quinolin-9-yl)-1,1-bis(pyridin-3-ylmethyl)thiourea (4d). Light gray crystals. Yield 53%, m.p. 178–180 °C. ¹H NMR, δ: 1.58–1.91 (m, 4 H, CH₂CH₂); 1.91–2.24 (m, 2 H, CH₂); 2.42–2.68 (m, 2 H, CH₂); 2.68–3.15 (m, 6 H, CH₂); 5.11 (c, 4 H, N(CH₂)₂); 6.84 (br.s, 1 H, NH); 7.36–7.43 (m, 2 H, pyridyl); 7.70–7.82 (m, 2 H, pyridyl); 8.54–8.71 (m, 4 H, pyridyl); 7.81 (br.s, 2 H, NH); 7.95 (d, 1 H, pyridyl, *J* = 7.8 Hz). Found (%): C, 69.77; H, 6.21; N, 16.45. C₂₅H₂₇N₅S. Calculated (%): C, 69.90; H, 6.34; N, 16.30.

Study of the esterase profile. The kinetic measurements were carried out using commercial samples of human erythrocyte AChE, equine serum BChE, and porcine liver CES.^{40,41} The AChE and BChE activities were measured by the Ellman method⁴² (λ = 412 nm) using acetylthiocholine (1 mmol L⁻¹) and butyrylthiocholine (1 mmol L⁻¹) as substrates, respectively, as described in detail previously;⁴³ determination conditions: 100 mM phosphate buffer (pH 7.5), 25 °C. The CES activity was determined by spectrophotometry by monitoring the release of 4-nitrophenol (λ = 405 nm) using 4-nitrophenyl acetate (1 mmol L⁻¹) as the substrate;⁴³ determination conditions: 100 mM phosphate buffer (pH 8.0), 25 °C. The measurements were carried out with a FLUOstar OPTIMA microplate reader (BMG Labtech, Germany). The

compounds were dissolved in DMSO, the incubation mixture contained 2% solvent. The primary evaluation of the inhibitory activity was carried out by determining the degree of enzyme inhibition at the compound concentration of $20 \mu\text{mol L}^{-1}$. For this purpose, the sample of the corresponding enzyme was incubated with the test compound for 5 min, and then the residual enzyme activity was measured. Each experiment was conducted in triplicate. For compounds that inhibited the enzyme by more than 30%, the IC_{50} values were determined, that is, the inhibitor concentration required to decrease the enzyme activity by 50%. The IC_{50} values for the AChE, BChE, and CES inhibition were found by incubating a sample of the enzyme with a test compound in the concentration range of $1 \cdot 10^{-12}$ – $1 \cdot 10^{-4} \text{ mol L}^{-1}$ for 5 min followed by measuring the residual enzyme activity. Each experiment was conducted in triplicate.

Study of the compounds as potential inhibitors of AChE-induced aggregation of β -amyloid. The test compounds were evaluated as potential inhibitors of the pro-aggregant activity of AChE by determining the degree of displacement of propidium iodide from the AChE PAS by the reported fluorescence method³⁰ with minor changes, as described in detail previously.⁴⁴ AChE from *Electrophorus electricus* (EeAChE) was used as the source of the enzyme.

Inhibition of $\text{A}\beta_{42}$ self-aggregation. The inhibitory activity of the test compounds against the self-aggregation of $\text{A}\beta_{42}$ was determined by the fluorescence method involving thioflavin T (ThT)^{31,32} with minor changes. The method is based on the specific interaction of a fluorescence dye, thioflavin T, with the β -folded structures formed upon self-aggregation of β -amyloid fibrils, which results in a considerable increase in the fluorescence intensity of the bound dye.⁴⁵ The decrease in the fluorescence signal in the presence of test compounds correlates with their inhibitory effect against the formation of $\text{A}\beta_{42}$ aggregates.

Commercially available freeze-dried $\text{A}\beta_{42}$ specimen treated with hexafluoroisopropyl alcohol (HFIP) (rPeptide, USA) was dissolved in DMSO to prepare the stable stock solution ($[\text{A}\beta_{42}] = 500 \mu\text{mol L}^{-1}$), the solution was aliquoted and stored at $-20 \text{ }^\circ\text{C}$. For evaluation of the self-aggregation of $\text{A}\beta_{42}$ and the degree of its inhibition by the test compounds, an aliquot of the prepared β -amyloid solution was dissolved in 215 mM Na phosphate buffer (pH 8.0) up to a final $\text{A}\beta_{42}$ concentration of $50 \mu\text{mol L}^{-1}$. Then the samples were incubated for 24 h at $37 \text{ }^\circ\text{C}$ in a thermostat without stirring in the absence (base level of $\text{A}\beta_{42}$ self-aggregation; control) or in the presence of test compounds. Myricetin was used as the reference compound. The final concentrations of all test compounds were $100 \mu\text{mol L}^{-1}$. After incubation, a solution of thioflavin T ($5 \mu\text{M}$) in glycine–NaOH buffer (pH 8.5) (50 mM) was added, and a fluorescence spectrum ($\lambda_{\text{ex}} = 440 \text{ nm}$, $\lambda_{\text{em}} = 485 \text{ nm}$) was recorded. The background fluorescence level of the solvent and the test compounds was taken into account by preparing control samples that contained 215 mM Na phosphate buffer (pH 8.0) and DMSO or test compounds, respectively. The measurements were carried

out with a FLUOstar OPTIMA multifunctional microplate reader (BMG Labtech, Germany). All measurements were conducted in triplicate; the results are expressed as mean \pm SEM.

The degree of inhibition of $\text{A}\beta_{42}$ self-aggregation by the test compounds (%) was calculated by the following relation:

$$\text{Degree of inhibition} = 100 - (\text{IF}_{\text{A}\beta+\text{inhibitor}}/\text{IF}_{\text{A}\beta}) \cdot 100\%,$$

where $\text{IF}_{\text{A}\beta}$ and $\text{IF}_{\text{A}\beta+\text{inhibitor}}$ are the fluorescence intensity in the absence of test compounds (taken as 100%) and in the presence of a test compound after subtraction of the fluorescence found in the corresponding control experiments, respectively.

Study of the antiradical activity of the test compounds. The antiradical activity of the compounds was determined by measuring their free radical-scavenging ability in the ABTS assay according to the known method³⁷ with minor modifications, as described in detail previously.⁴⁴ The test compounds were dissolved in DMSO, the content of which in the reaction mixture was 4% (by volume), $\text{ABTS}^{\cdot+}$ was added to the solution (the final $\text{ABTS}^{\cdot+}$ concentration in the reaction mixture was $100 \mu\text{mol L}^{-1}$), and the solution was thoroughly stirred. The reaction was carried out at $30 \text{ }^\circ\text{C}$ in the dark; the incubation time was 1 h. The degree of bleaching of the $\text{ABTS}^{\cdot+}$ solution was determined at 734 nm with an xMark microplate reader (BioRad, USA). The compounds were tested in the concentration range of $1 \cdot 10^{-6}$ – $1 \cdot 10^{-4} \text{ mol L}^{-1}$. All measurements were conducted in triplicate for three independent experiments.

The antiradical activity was expressed in the TEAC units, found as the ratio of the slopes of the plots for decreasing concentration of the $\text{ABTS}^{\cdot+}$ radical *versus* concentrations of the test compound and trolox. For all compounds, IC_{50} values were also determined (concentration of the compound at which the $\text{ABTS}^{\cdot+}$ concentration decreases by 50%). The calculations were carried out using the Origin 6.1 program for Windows (OriginLab, USA). All results are expressed as mean values \pm SEM, calculated using the GraphPad Prism program, version 6.05 for Windows (GraphPad Software, USA).

Study of the iron-reducing activity of the test compounds (FRAP method). The FRAP method is based on the reduction of the $[\text{Fe}^{3+}-(\text{TPTZ})_2]^{3+}$ complex in the presence of antioxidant to give $[\text{Fe}^{2+}-(\text{TPTZ})_2]^{2+}$, which is intensely blue-colored with the absorption maximum at $\lambda = 593 \text{ nm}$.^{38,46} The method was modified to be implemented in a 96-well plate and described in detail in our previous study.⁴³ The FRAP reagent was prepared by mixing a 0.3 M acetate buffer (pH 3.6), 10 mM solutions of 2,4,6-tris(pyridin-2-yl)-1,3,5-triazine (TPTZ) in 40 mM HCl and 20 mM $\text{FeCl}_3 \cdot 6\text{H}_2\text{O}$ in water in 10 : 1 : 1 ratio (v/v/v) directly prior to use. The compounds were dissolved in DMSO and studied in the concentration range of $1 \cdot 10^{-6}$ – $1 \cdot 10^{-4} \text{ mol L}^{-1}$. The concentration of the solvent in the reaction mixture was 4% (v/v). A solution of a test compound ($10 \mu\text{L}$) was added to the solution of the FRAP reagent ($240 \mu\text{L}$) and the mixture was thoroughly stirred. The reaction was carried out at $37 \text{ }^\circ\text{C}$ in

the dark; the incubation time was 1 h. The reaction was monitored by measuring the change in the absorbance at 600 nm using a FLUOStar OPTIMA microplate reader with respect to the control containing all components except for $\text{FeCl}_3 \cdot 6\text{H}_2\text{O}$. Trolox was used as the standard. All measurements were carried out in triplicate for three independent experiments. The iron-reducing capacity of the compounds is expressed in relative units, trolox equivalents (TE), which are calculated as the ratio of trolox and test compound concentrations that induce equal effects.

Molecular modeling. $\text{p}K_a$ values for the amiridine moiety were estimated using the Marvin 21.14 module of the ChemAxon program package (<http://www.chemaxon.com>) and the MolGpka web service (<https://xundrug.cn/molgpka>).⁴⁷ The ligand structures were optimized for molecular docking by quantum mechanics (DFT method (B3LYP/6-31G*), the GAMESS-US program).⁴⁸ The partial atomic charges were derived from the quantum mechanical data using the Löwdin scheme.⁴⁹ The following crystallographic structures were used as targets for molecular docking: PDB ID 4EY7 for AChE⁵⁰ (the choice of the method for determination of the partial atomic charges and AChE crystallographic structure was substantiated⁵¹ and the structure preparation was described in detail⁵² previously); PDB ID 1P0I for BChE⁵³ (the structure preparation was described in detail previously⁵⁴), and PDB ID 1IYT for $\text{A}\beta_{42}$.⁵⁵ All conformers were used; hydrogen atoms were added according to the pH of the solution (pH 7.4) using $\text{p}K_a$ estimates made by PropKa web service (<https://www.ddl.unimi.it/vegaol/propka.htm>)⁵⁶).

Molecular docking was performed using Lamarckian Genetic Algorithm (LGA⁵⁷) and Autodock 4.2.6 software.⁵⁸ The docking grid with a spacing of 0.375 Å was taken for all targets; the grid included the whole active sites of AChE (22.5×22.5×22.5 Å³ grid box) and BChE (15×20.25×18 Å³ grid box). For all conformers of $\text{A}\beta_{42}$, the grid box had dimensions 43.5×28.5×54.75 Å³ and included each conformer entirely. The main LGA parameters were chosen as 256 runs, $27 \cdot 10^4$ generations, population size of 3000, and $25 \cdot 10^6$ evaluations. The best positions in the binding energy were used for analysis.

The three-dimensional structural images were prepared using the PyMol software (<https://pymol.org/>).

The study was carried out within the state assignment of the Institute of Physiologically Active Compounds, Russian Academy of Sciences (No. FFSN-2021-0005) and was partially supported by the Russian Foundation for Basic Research (Project No. 19-53-26016a). Molecular modeling was carried out using the shared research facilities of the HPC computing resources at Lomonosov Moscow State University.

No human or animal subjects were used in this research.

The authors declare no competing interests.

References

1. J. Cummings, G. Lee, A. Ritter, M. Sabbagh, K. Zhong, *Alzheimer's Dementia*, 2019, **5**, 272; DOI: 10.1016/j.trci.2019.05.008.
2. M. C. Carreiras, E. Mendes, M. J. Perry, A. P. Francisco, J. Marco-Contelles, *Curr. Top. Med. Chem.*, 2013, **13**, 1745; DOI: 10.2174/15680266113139990135.
3. Y. Huang, L. Mucke, *Cell*, 2012, **148**, 1204; DOI: 10.1016/j.cell.2012.02.040.
4. L. Ismaili, B. Refouvet, M. Bencheikroun, S. Brogi, M. Brindisi, S. Gemma, G. Campiani, S. Filipic, D. Agbaba, G. Esteban, M. Unzeta, K. Nikolic, S. Butini, J. Marco-Contelles, *Prog. Neurobiol.*, 2017, **151**, 4; DOI: 10.1016/j.pneurobio.2015.12.003.
5. K. Spilovska, J. Korabecny, E. Nepovimova, R. Dolezal, E. Mezirova, O. Soukup, K. Kuca, *Curr. Top. Med. Chem.*, 2017, **17**, 1006; DOI: 10.2174/1568026605666160927152728.
6. F. Mesiti, D. Chavarria, A. Gaspar, S. Alcaro, F. Borges, *Eur. J. Med. Chem.*, 2019, **181**, 111572; DOI: 10.1016/j.ejmech.2019.111572.
7. M. Girek, P. Szymański, *Chem. Pap.*, 2019, **73**, 269; DOI: 10.1007/s11696-018-0590-8.
8. R. T. Kareem, F. Abedinifar, E. A. Mahmood, A. G. Ebadi, F. Rajabi, E. Vessally, *RSC Adv.*, 2021, **11**, 30781; DOI: 10.1039/d1ra03718h.
9. E. E. Bukatina, I. V. Grigor'eva, E. I. Sokol'chik, *Neurosci. Behav. Physiol.*, 1993, **23**, 83; DOI: 10.1007/BF01182643.
10. V. Kluša, J. Rumaks, Ņ. Karajeva, *Proc. Latv. Acad. Sci., Sect. B*, 2008, **62**, 85; DOI: 10.2478/v10046-008-0024-z.
11. I. V. Damulin, D. A. Stepkina, A. B. Lokshina, *Zhurn. Nevrologii i Psikiatrii im. S. S. Korsakova [S. S. Korsakov J. Neurol. and Psych.]*, 2011, **111**, No. 2, 40 (in Russian).
12. S. A. Zhivolupov, L. S. Onishchenko, N. A. Rashidov, I. N. Samartsev, E. V. Yakovlev, *Zhurn. Nevrologii i Psikiatrii im. S. S. Korsakova [S. S. Korsakov J. Neurol. and Psych.]*, 2018, **118**, No. 2, 58–64; DOI: 10.17116/jnevro20181182158-64 (in Russian).
13. M. M. Oros, *Int. J. Neurol.*, 2018, 23; DOI: 10.22141/2224-0713.6.100.2018.146454.
14. I. V. Litvinenko, S. A. Zhivolupov, I. N. Samartsev, A. Y. Kravchuk, M. N. Vorobyova, E. V. Yakovlev, Y. S. Butakova, *Neurosci. Behav. Physiol.*, 2020, **50**, 1112; DOI: 10.1007/s11055-020-01012-y.
15. J. Kojima, K. Onodera, M. Ozeki, K. Nakayama, *CNS Drug Rev.*, 1998, **4**, 247; DOI: 10.1111/j.1527-3458.1998.tb00067.x.
16. P. N. Shevtsov, E. F. Shevtsova, G. Sh. Burbaeva, S. O. Bachurin, *Bull. Exp. Biol. Med.*, 2014, **156**, 768; DOI: 10.1007/s10517-014-2445-9.
17. G. F. Makhaeva, S. V. Lushchekina, N. V. Kovaleva, T. Yu. Astakhova, N. P. Boltneva, E. V. Rudakova, O. G. Serebryakova, A. N. Proshin, I. V. Serkov, T. P. Trofimova, V. A. Tafeenko, E. V. Radchenko, V. A. Palyulin, V. P. Fisenko, J. Korábečný, O. Soukup, R. J. Richardson,

- Bioorg. Chem.*, 2021, **112**, 104974; DOI: 10.1016/j.bioorg.2021.104974.
18. S. Yoshida, N. Suzuki, *Eur. J. Pharmacol.*, 1993, **250**, 117; DOI: 10.1016/0014-2999(93)90628-u.
19. A. M. Zhidkova, A. S. Berlyand, A. Z. Knizhnik, E. F. Lavretskaya, T. N. Robakidze, S. A. Sukhanova, T. P. Mufazalova, *Pharm. Chem. J.*, 1989, **23**, 709; DOI: 10.1007/BF00764431.
20. A. M. Zhidkova, M. S. Goizman, A. S. Berlyand, A. Z. Knizhnik, L. S. Khabarova, *Khim.-Farm. Zhurn. [Pharm. Chem. J.]*, 1989, **23**, 1401 (in Russian).
21. G. F. Makhaeva, N. V. Kovaleva, N. P. Boltneva, E. V. Rudakova, S. V. Lushchekina, T. Y. Astakhova, I. V. Serkov, A. N. Proshin, E. V. Radchenko, V. A. Palyulin, J. Korabecny, O. Soukup, S. O. Bachurin, R. J. Richardson, *Molecules*, 2022, **27**, 1060; DOI: 10.3390/molecules27031060.
22. S. Bachurin, S. Tkachenko, I. Baskin, N. Lermontova, T. Mukhina, L. Petrova, A. Ustinov, A. Proshin, V. Grigoriev, N. Lukoyanov, V. Palyulin, N. Zefirov, *Ann. N. Y. Acad. Sci.*, 2001, **939**, 219; DOI: 10.1111/j.1749-6632.2001.tb03629.x.
23. G. L. Perlovich, A. N. Proshin, T. V. Volkova, S. V. Kurkov, V. V. Grigoriev, L. N. Petrova, S. O. Bachurin, *J. Med. Chem.*, 2009, **52**, 1845; DOI: 10.1021/jm8012882.
24. H. Pavan Kumar, H. K. Kumara, R. Suhas, D. Channe Gowda, *Arch. Pharm.*, 2021, **354**, e2000468; DOI: 10.1002/ardp.202000468.
25. B. Ozgeris, *J. Antibiot.*, 2021, **74**, 233; DOI: 10.1038/s41429-020-00399-7.
26. D. Q. Huong, M. V. Bay, P. C. Nam, *J. Mol. Liq.*, 2021, **340**, 117149; DOI: 10.1016/j.molliq.2021.117149.
27. M. Bajda, S. Filipek, *Bioorg. Med. Chem. Lett.*, 2017, **27**, 212; DOI: 10.1016/j.bmcl.2016.11.072.
28. T. Mohamed, P. P. N. Rao, *Eur. J. Med. Chem.*, 2017, **126**, 823; DOI: 10.1016/j.ejmech.2016.12.005.
29. G. F. Makhaeva, E. V. Rudakova, N. V. Kovaleva, S. V. Lushchekina, N. P. Boltneva, A. N. Proshin, E. V. Shchegolkov, Ya. V. Burgart, V. I. Saloutin, *Russ. Chem. Bull.*, 2019, **68**, 967; DOI: 10.1007/s11172-019-2507-2.
30. P. Taylor, S. Lappi, *Biochemistry*, 1975, **14**, 1989; DOI: 10.1021/bi00680a029.
31. M. Bartolini, C. Bertucci, V. Cavrini, V. Andrisano, *Biochem. Pharmacol.*, 2003, **65**, 407; DOI: 10.1016/s0006-2952(02)01514-9.
32. P. Munoz-Ruiz, L. Rubio, E. Garcia-Palomero, I. Dorronsoro, M. Del Monte-Millan, R. Valenzuela, P. Usan, C. De Austria, M. Bartolini, V. Andrisano, A. Bidon-Chanal, M. Orozco, F. J. Luque, M. Medina, A. Martinez, *J. Med. Chem.*, 2005, **48**, 7223; DOI: 10.1021/jm0503289.
33. H. Safarizadeh, Z. Garkani-Nejad, *J. Mol. Graph. Model.*, 2019, **87**, 129; DOI: 10.1016/j.jmgm.2018.11.019.
34. S. Jokar, M. Erfani, O. Bavi, S. Khazaee, M. Sharifzadeh, M. Hajiramezanali, D. Beiki, A. Shamloo, *Bioorg. Chem.*, 2020, **102**, 104050; DOI: 10.1016/j.bioorg.2020.104050.
35. J. Wang, P. Cai, X.-L. Yang, F. Li, J.-J. Wu, L.-Y. Kong, X.-B. Wang, *Eur. J. Med. Chem.*, 2017, **139**, 68; DOI: 10.1016/j.ejmech.2017.07.077.
36. M. P. Williamson, Y. Suzuki, N. T. Bourne, T. Asakura, *Biochem. J.*, 2006, **397**, 483; DOI: 10.1042/BJ20060293.
37. R. Re, N. Pellegrini, A. Proteggente, A. Pannala, M. Yang, C. Rice-Evans, *Free Radical Biol. Med.*, 1999, **26**, 1231; DOI: 10.1016/s0891-5849(98)00315-3.
38. I. F. F. Benzie, J. J. Strain, *Methods Enzymol.*, 1999, **299**, 15; DOI: 10.1016/s0076-6879(99)99005-5.
39. S. Meir, J. Kanner, B. Akiri, S. Philosoph-Hadas, *J. Agric. Food Chem.*, 1995, **43**, 1813; DOI: 10.1021/jf00055a012.
40. G. F. Makhaeva, E. V. Radchenko, V. A. Palyulin, E. V. Rudakova, A. Yu. Aksinenko, V. B. Sokolov, N. S. Zefirov, R. J. Richardson, *Chem.-Biol. Interact.*, 2013, **203**, 231; DOI: 10.1016/j.cbi.2012.10.012.
41. G. F. Makhaeva, E. V. Rudakova, O. G. Serebryakova, A. Yu. Aksinenko, S. V. Lushchekina, S. O. Bachurin, R. J. Richardson, *Chem.-Biol. Interact.*, 2016, **259**, 332; DOI: 10.1016/j.cbi.2016.05.002.
42. G. L. Ellman, K. D. Courtney, V. Andres, Jr., R. M. Feather-Stone, *Biochem. Pharmacol.*, 1961, **7**, 88; DOI: 10.1016/0006-2952(61)90145-9.
43. G. F. Makhaeva, N. V. Kovaleva, N. P. Boltneva, S. V. Lushchekina, T. Yu. Astakhova, E. V. Rudakova, A. N. Proshin, I. V. Serkov, E. V. Radchenko, V. A. Palyulin, S. O. Bachurin, R. J. Richardson, *Molecules*, 2020, **25**, 3915; DOI: 10.3390/molecules25173915.
44. G. F. Makhaeva, N. V. Kovaleva, N. P. Boltneva, S. V. Lushchekina, E. V. Rudakova, T. S. Stupina, A. A. Terentiev, I. V. Serkov, A. N. Proshin, E. V. Radchenko, V. A. Palyulin, S. O. Bachurin, R. J. Richardson, *Bioorg. Chem.*, 2020, **94**, 103387; DOI: 10.1016/j.bioorg.2019.103387.
45. M. Biancalana, S. Koide, *Biochim. Biophys. Acta, Proteins Proteom.*, 2010, **1804**, 1405; DOI: 10.1016/j.bbapap.2010.04.001.
46. I. F. Benzie, J. J. Strain, *Anal. Biochem.*, 1996, **239**, 70; DOI: 10.1006/abio.1996.0292.
47. X. Pan, H. Wang, C. Li, J. Z. H. Zhang, C. Ji, *J. Chem. Inf. Model.*, 2021, **61**, 3159; DOI: 10.1021/acs.jcim.1c00075.
48. M. W. Schmidt, K. K. Baldridge, J. A. Boatz, S. T. Elbert, M. S. Gordon, J. H. Jensen, S. Koseki, N. Matsunaga, K. A. Nguyen, S. Su, T. L. Windus, M. Dupuis, J. A. Montgomery, *J. Comput. Chem.*, 1993, **14**, 1347; DOI: 10.1002/jcc.540141112.
49. P.-O. Löwdin, in *Advances in Quantum Chemistry*, Ed. P.-O. Löwdin, Academic Press, New York, London, 1970, p. 185.
50. J. Cheung, M. J. Rudolph, F. Burshteyn, M. S. Cassidy, E. N. Gary, J. Love, M. C. Franklin, J. J. Height, *J. Med. Chem.*, 2012, **55**, 10282; DOI: 10.1021/jm300871x.
51. S. V. Lushchekina, G. F. Makhaeva, D. A. Novichkova, I. V. Zueva, N. V. Kovaleva, R. J. Richardson, *Supercomput. Front. Innov.*, 2018, **5**, 89; DOI: 10.14529/jsfi1804.

52. I. Zueva, S. Lushchekina, P. Shulnikova, O. Lenina, K. Petrov, E. Molochkina, P. Masson, *Chem. Biol. Interact.*, 2021, **348**, 109646; DOI: 10.1016/j.cbi.2021.109646.
53. Y. Nicolet, O. Lockridge, P. Masson, J. C. Fontecilla-Camps, F. Nachon, *J. Biol. Chem.*, 2003, **278**, 41141; DOI: 10.1074/jbc.M210241200.
54. P. Masson, S. Lushchekina, L. M. Schopfer, O. Lockridge, *Biochem. J.*, 2013, **454**, 387; DOI: 10.1042/bj20130389.
55. O. Crescenzi, S. Tomaselli, R. Guerrini, S. Salvadori, A. M. D'Ursi, P. A. Temussi, D. Picone, *Eur. J. Biochem.*, 2002, **269**, 5642; DOI: 10.1046/j.1432-1033.2002.03271.x.
56. H. Li, A. D. Robertson, J. H. Jensen, *Proteins*, 2005, **61**, 704; DOI: 10.1002/prot.20660.
57. G. M. Morris, D. S. Goodsell, R. S. Halliday, R. Huey, W. E. Hart, R. K. Belew, A. J. Olson, *J. Comput. Chem.*, 1998, **19**, 1639; DOI: 10.1002/(sici)1096-987x(19981115)19:14<1639::aid-jcc10>3.0.co;2-b.
58. G. M. Morris, R. Huey, W. Lindstrom, M. F. Sanner, R. K. Belew, D. S. Goodsell, A. J. Olson, *J. Comput. Chem.*, 2009, **30**, 2785; DOI: 10.1002/jcc.21256.

Received June 1, 2022;
in revised form August 2, 2022;
accepted August 15, 2022